

Green Chemistry

Accepted Manuscript



This is an *Accepted Manuscript*, which has been through the Royal Society of Chemistry peer review process and has been accepted for publication.

Accepted Manuscripts are published online shortly after acceptance, before technical editing, formatting and proof reading. Using this free service, authors can make their results available to the community, in citable form, before we publish the edited article. We will replace this *Accepted Manuscript* with the edited and formatted *Advance Article* as soon as it is available.

You can find more information about *Accepted Manuscripts* in the [Information for Authors](#).

Please note that technical editing may introduce minor changes to the text and/or graphics, which may alter content. The journal's standard [Terms & Conditions](#) and the [Ethical guidelines](#) still apply. In no event shall the Royal Society of Chemistry be held responsible for any errors or omissions in this *Accepted Manuscript* or any consequences arising from the use of any information it contains.

One-pot extraction combined with metal-free photochemical aerobic oxidative desulfurization in deep eutectic solvent

Wenshuai Zhu ^{*[a]}, Chao Wang ^[a], Hongping Li ^[a], Peiwen Wu, ^[a] Suhang Xun, ^[a] Wei Jiang ^[b], Zhigang Chen ^[a], Zhen Zhao ^[c] and Huaming Li ^{*[b]}

^[a]School of Chemistry and Chemical Engineering, Jiangsu University, 301 Xuefu Road, Zhenjiang 212013 (P. R. China)

^[b] Insititute for Energy Research, Jiangsu University, 301 Xuefu Road, Zhenjiang 212013 (P. R. China)

^[c] State Key Laboratory of Heavy Oil Processing, Faculty of Science, China University of Petroleum, Beijing 102249 (P. R. China)

E-mail: zhuws@ujs.edu.cn (W.S. Zhu) , lhm@ujs.edu.cn (H.M. Li)

Abstract: Five low-cost deep eutectic solvents (DESs) were synthesized based on choline chloride (ChCl) and a series of straight-chain monobasic acids. Under UV light irradiation, one-pot extraction combined with metal-free photochemical aerobic oxidative deep desulfurization of fuels in deep eutectic solvents was successfully achieved. This liquid-liquid extraction and photochemical oxidative desulfurization system (EPODS) composed of air, isobutylaldehyde (IBA), DESs and model oil. The influence factors on sulfur removal were systematically investigated, including the amount of DES, volume ratio of model oil and IBA, different sulfur concentration, different substrates and fuel composition. Sulfur removal of dibenzothiophene (DBT) could reach 98.6% with air as oxidizing agent under UV light irradiation. Sulfur

removal of different sulfur compounds decreased as: BT > DBT > 4,6-DMDBT. The possible photochemical oxidative desulfurization mechanism was researched by Gas chromatograph-mass Spectrometer (GC-MS), electron spin-resonance (ESR) spectroscopy and density functional theory (DFT).

Keywords: metal-free, deep eutectic solvents, oxidative desulfurization, photochemical,

Introduction

Organic sulfur compounds exist in fuels have aroused worldwide concerns, as SO_x would produce after combustion in automobiles, leading to acid rain, haze or many other environmental issues.^{1,2} Thus, many countries have promulgated regulations to restrict sulfur content in fuels.³ Hydrodesulfurization (HDS) is one of the most mature technologies in modern industry, sulfur compounds could convert to H_2S in the high temperature, high pressure and hydrogen filled environment with CoMo or NiMo as catalysts.⁴ However, thiophene-analogue sulfur compounds, such as benzothiophene (BT), dibenzothiophene (DBT), 4,6-dimethyldibenzothiophene (4,6-DMDBT), have low reaction activities in the above reaction environment, as their stereo hindrance and many other reasons.⁵⁻⁷ Besides this, the harsh reaction conditions not only made the reaction apparatus easy to be damaged, but also caused a great loss in the octane of fuels.⁸ Therefore, the more suitable method for deep desulfurization in moderate reaction environment is seeking, and many energy-efficient and charge-effective technologies have gained.⁹⁻¹¹

Compared with other non-HDS methods, such as adsorption desulfurization

(ADS),¹²⁻¹⁴ extraction desulfurization (EDS)¹⁵⁻¹⁷ and biodesulfurization¹⁸, oxidative desulfurization (ODS) is one of the most promising methods as its moderate reaction environment, high desulfurization and intact octane number compared to HDS.^{5, 19-21} Many classical oxidants include oxygen²¹⁻²⁴, hydrogen peroxide²⁵⁻²⁹, ozone^{30, 31}, organic hydroperoxide³² have been reported, in which molecular oxygen is the most green and low-cost oxidant. However, its triplet ground state makes it inactive in many redox reactions.³³ Some metal^{5, 34, 35} and metal-free²⁴ catalysts are designed to have the ability to activate O₂ in desulfurization reaction system. But, these reactions were undergone in the high temperature or high pressure or long time reaction environment. Consideration of these problems, photochemical method could be introduced in oxidative desulfurization and it was also regarded as an effective and burgeoning desulfurization technique. The reported photocatalysts in oxidative desulfurization usually included metal-containing photocatalysts, such as Pt-RuO₂/BiVO₄³⁶, Pt-RuO₂/TiO₂³⁷, Triton X-100/TiO₂³⁸, IL/TiO₂^{39, 40}, carbon nanotubes/TiO₂⁴¹, C₃N₄/TiO₂⁴² and Fe₂O₃⁴³, *etc.*. From the standpoint of sustainable and green chemistry, the development of metal-free photochemical systems in oxidative desulfurization is a promising technology. Aldehyde as a kind of hydrocarbon not only fails to contaminate oil, but also contributes to the heat of oil combustion, which can be used in aerobic oxidative desulfurization system under the irradiation of light³³.

Additionally, as an effective ODS method, our group have developed ILs extraction coupled catalytic oxidative desulfurization system (ECODS) and exhibited

deep desulfurization performance⁴⁴⁻⁴⁶. To date, most reports of ECODS were operated under thermocatalytic conditions and with explosive H₂O₂ as oxidant. What's more, the industrial application of ILs are rarely existed which is limited by its high cost, purification difficulty and low biodegradability.⁴⁷ Deep eutectic solvents (DESs), as ILs analogues, have been developed.⁴⁸⁻⁵⁶ These greener solvents are composed of hydrogen-bond acceptor (HBA) (as ammonium or phosphonium salt, *etc*) with hydrogen-bond donors (HBD) (as organic acid, urea, sugars, alcohols, *etc*)⁴⁸⁻⁵⁶, which not only share the merits of ionic liquids, but also present many other advantages such as low-cost, green and pristine synthesis route without separation and purification. In recent years, DESs solvents have been widely used in extraction⁵⁷, material preparation^{58, 59}, separation process^{60, 61}, substance dissolution⁶², electrochemistry⁶³, catalysis⁶⁴ and synthesis⁶⁵. Li et al.⁶⁶ reported on ammonium-based DESs for extraction dsulfurization of fuels. The extractive efficiency of these DESs is much higher than those of traditional and functionalized ILs, proving DES is a good extractant in desulfurization of fuels.

In this work, we find that isobutylaldehyde (IBA) can activate air under UV irradiation in DES. Hence, a simple liquid-liquid extraction and photochemical oxidative desulfurization system (EPODS) composed of air, isobutylaldehyde (IBA), and DES for the deep removal of sulfur compounds in model oil has been developed. EDSs were synthesized by a cheap and biodegradable choline chloride (ChCl) and a series of straight-chain monobasic acids. Sulfur compounds in model oil were extracted into DES phase and oxidized to their corresponding sulfones by air under

UV irradiation, achieving deep desulfurization. Here, we concluded that the innovation points in this work as following: (1) Use air as oxidant to replace explosive H_2O_2 . (2) Develop a metal-free photochemical oxidative desulfurization system. (3) Low-cost and greener DES was employed in one-pot EPODS under mild conditions.

Results and Discussion:

The characterization of DESs

To investigate the composition of DESs, elemental analyses of C, H, N of the as-prepared DESs were taken and the results were listed in Table S1. The experiment value of C, H and N elements were near the theoretical value, indicating no gaseous molecules was generated or evaporated out of the system.

FT-IR spectra of organic acid, ChCl and DESs ($\text{ChCl} \cdot 2\text{C}_n\text{H}_{2n+1}\text{COOH}$, $n=0, 1, 2, 3, 4$) were collected as shown in Fig. 1 and Fig. S1-Fig. S4. Compared with CH_3COOH and ChCl, redshift of peaks of $\text{C}=\text{O}$ (from 1728 cm^{-1} to 1720 cm^{-1}) and $\text{CH}_2\text{-CH}_2\text{-O}$ (from 1092 cm^{-1} to 1084 cm^{-1}) in $\text{ChCl} \cdot 2\text{CH}_3\text{COOH}$ were obviously seen (Fig. 1), indicating more stable H-bond were formed. However, redshift of $\text{C}=\text{O}$ in DESs gradually changed to blueshift with the carbon chain length of organic acid increased (Fig. S1 - Fig. S4). As is known to us all, organic acid usually existed in the morphology of dimers in the liquid phase, and as carbon chain length of organic acid increased, the H-bond of two acids becomes stronger. Because longer carbon chain induced stronger ultra-conjugated, then more negative charge would distribute in O atomic, and stronger H-bond would form at last. Strong H-bond between two acids changed to weak H-bond between ChCl and acids made the blueshift of $\text{C}=\text{O}$ in IR

spectra finally.

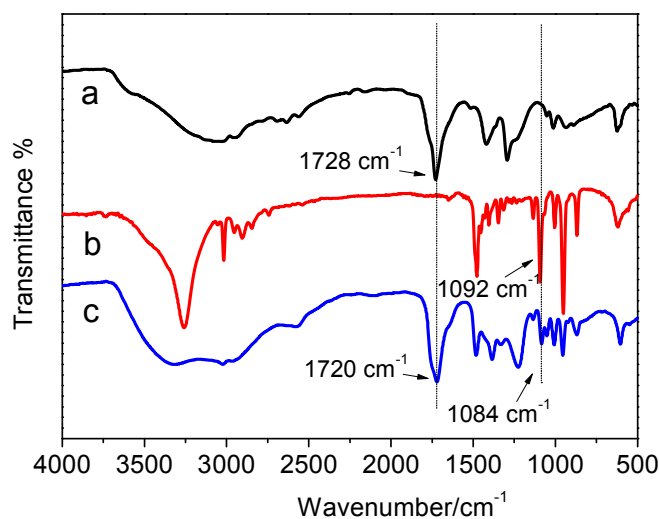


Fig. 1 FT-IR spectra of the as-prepared DES
a. CH₃COOH; b. ChCl; c. ChCl·2CH₃COOH

To further confirm the interactions were existed between ChCl and CH₃COOH, ¹H NMR spectra of ChCl, CH₃COOH and ChCl·2CH₃COOH were obtained as shown in Fig. S5-Fig S7 and Fig 2A. The most H peaks in DES were the same as H peaks in ChCl and CH₃COOH, expect the H peak of hydroxyl in ChCl and H peak of carboxyl in CH₃COOH. Here, the above two higher and narrower H peaks (11.9361 ppm, 5.7197 ppm) in Fig. 2B changed to shorter and wider peaks (12.0577 ppm, 5.6476 ppm) in Fig. 2C after the formation of DES. The reason for this is that the hydrogen bond of DES has been formed between the chloride anion and CH₃COOH.^{66, 67} Additionally, based on the integral value of H element in HNMR spectrum of Fig. S7, the molar ratio of ChCl and CH₃COOH was almost close to 2:1. It can be proved that no chemical transformation presented between ChCl and CH₃COOH, and the

chemical force between CH_3COOH and ChCl was hydrogen bond.

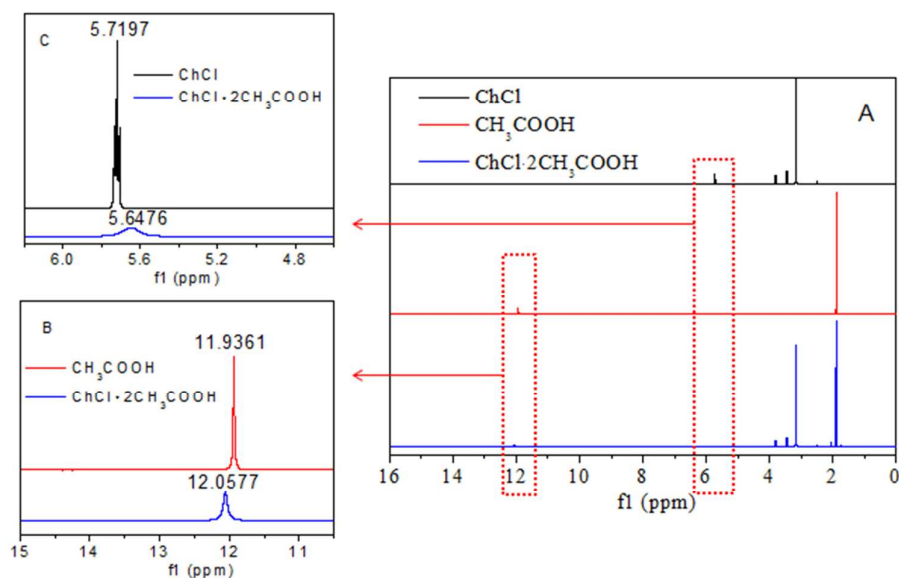


Fig 2 ^1H NMR of ChCl , CH_3COOH and $\text{ChCl}\cdot 2\text{CH}_3\text{COOH}$

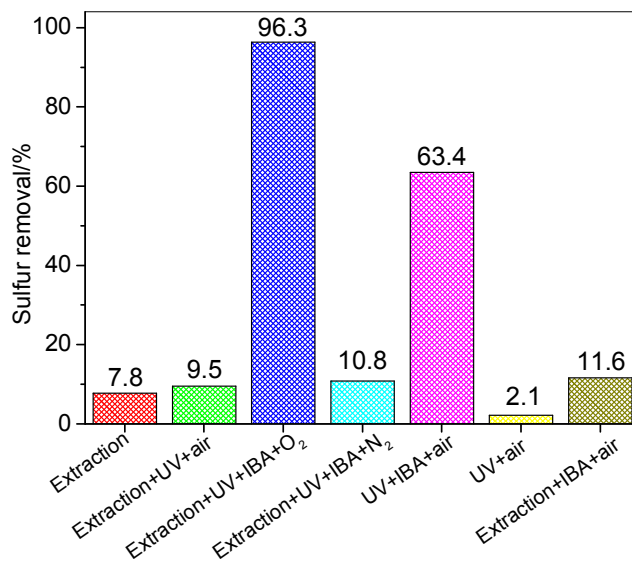


Fig. 3 Sulfur removal of different photochemical desulfurization systems in model oil

Experiment conditions: $T=30^\circ\text{C}$, $V(\text{model oil})=15\text{ mL}$, $V(\text{IBA})=200\ \mu\text{L}$, $t=3\text{ h}$,

$V_{\text{DES}}(\text{ChCl}\cdot 2\text{CH}_3\text{COOH})=3\text{ mL}$, $v(\text{air})=5\text{ mL/min}$

Fig. 3 depicts the removal of DBT in model oil in different reaction systems. Sulfur removals were very low under the reaction condition of only extraction (7.8%), only UV light irradiation (2.1%) and the combination of extraction and UV light irradiation (9.5%) with air as oxidant. Though aerobic oxidative sulfur removal could reach to 63.4% when IBA was added to model oil under UV irradiation, it still failed to reach deep desulfurization. However, when DES was added into the system above, forming EPODS, sulfur removal increased sharply, reaching 96.3% and achieving deep desulfurization. In addition, when air was replaced by N₂ in above EPODS, sulfur removal decreased obviously to 10.8%. These results indicated that IBA can transform into active oxidizing species with air under the UV light irradiation and both DES as extractant and air as oxidant played important roles in desulfurization reaction process. Meanwhile, sulfur removal dropped to 11.6% without UV light irradiation, which indicated UV light irradiation also played a decisive role in oxidative desulfurization.

Structure-activity relationship of desulfurization

Table 1. Sulfur removal of model oil in different hydrogen bond donors

Entry	ChCl·2HA	Extraction ability (%)	Sulfur removal (%)
1	ChCl·2HCOOH	5.2	68.7
2	ChCl·2CH ₃ COOH	8.8	96.4
3	ChCl·2C ₂ H ₅ COOH	7.8	91.6
4	ChCl·2C ₃ H ₇ COOH	5.8	66.5
5	ChCl·2C ₄ H ₉ COOH	3.4	42.5

Experiment condition: T=30°C, V(model oil)=15 mL, V(IBA)= 200 μL, t= 3 h, V(DES)= 3 mL, v(air)=5 mL/min, HA: Organic acids.

Sulfur removals of extraction (2.6~8.8%) and EPODS (22.3~96.4%) with different DESs were recorded in Table 1. Among five DESs, sulfur removal of extraction with $\text{ChCl}\cdot 2\text{CH}_3\text{COOH}$ as well as EPODS, reaching 8.8% and 96.4%, respectively. The DES synthesized by long carbon organic acids showed a decrease extraction ability of DBT on the whole. Sulfur removals of EPODS decreased with carbon chain of hydrogen bond donor increasing except $\text{ChCl}\cdot 2\text{HCOOH}$. The same rule could be found in extraction and EPODS. Based on the above results, $\text{ChCl}\cdot 2\text{HCOOH}$ was used as DES in the further investigation.

Optimization of oxidative desulfurization parameters

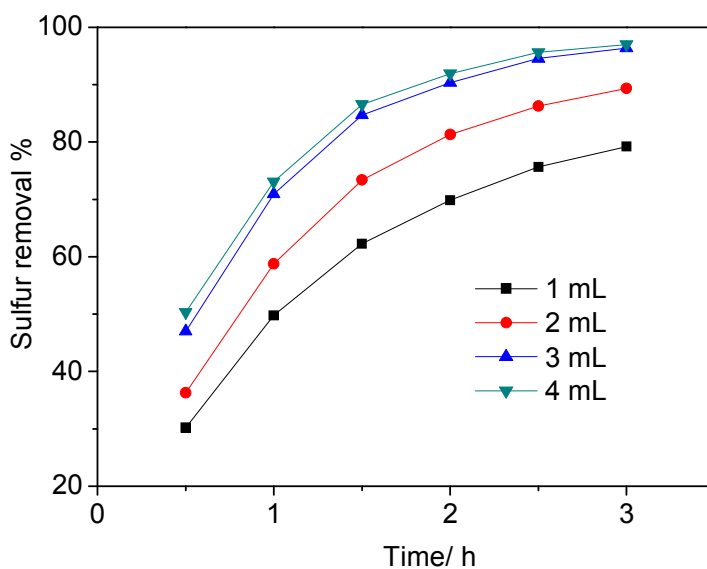


Fig. 4 Influence of the amount of DES on the removal of DBT.

Experiment conditions: $T=30^{\circ}\text{C}$, $V(\text{model oil})=15\text{ mL}$, $V(\text{IBA})=200\ \mu\text{L}$, $v(\text{air})=5\text{ mL/min}$

Fig. 4 shows that the volume of DES plays very important role in this reaction. When the amount of DES increased from 1 mL to 4 mL, sulfur removal increased from 79.2% to 97.0% accordingly. However, when the volume of DES was 3 mL sulfur removal could reach to 96.3%, which was slight lower than that of 4 mL DES. Finally, the use of 3 mL DES was chosen as the optimized value in the following investigation.

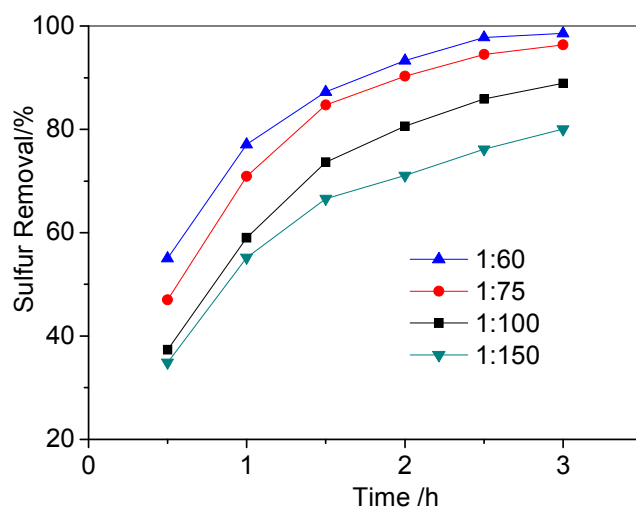


Fig. 5 Effect of volume ratio of IBA and model oil on the removal of DBT.
Experiment conditions: $T=30^{\circ}\text{C}$, $V(\text{model oil})=15\text{ mL}$, $V(\text{DES})=3\text{ mL}$, $v(\text{air})=5\text{ mL/min}$

The amount of IBA added in the reaction system also affected desulfurization efficiency. Thus, sulfur removal with different amount of IBA addition was plotted. As can be seen from Fig. 5, when the volume ratio of IBA and model oil increased from 1:150 to 1:60, sulfur removal of DBT in model oil changed from 80.1% to 98.6%. As deep desulfurization was achieved, addition of IBA (volume ratio of IBA

and model oil equal to 1:75) was chosen as the appropriate amount in this reaction system.

Sulfur removal of DBT with different S-concentration

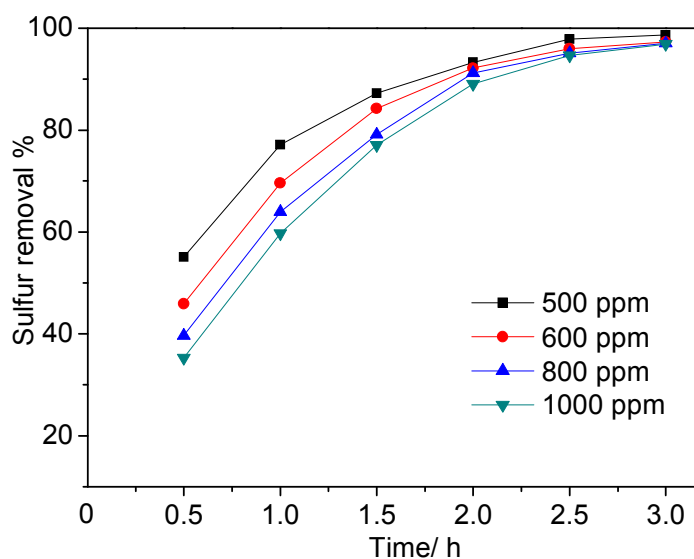


Fig 6. Sulfur removal of DBT with different S-concentration.
Experiment condition: $T=30^{\circ}\text{C}$, $V(\text{model oil})=15\text{ mL}$, $V(\text{IBA})=250\ \mu\text{L}$,
 $V(\text{DES})=3\text{ mL}$, $v(\text{air})=5\text{ mL/min}$

Considering the deep desulfurization for various oils in applications, model oils with different S-content were tested under the same reaction conditions (Fig. 6). Though sulfur removal of high S-content model oil was much lower than that of 500 ppm S-content oil, sulfur removal with different S-content model oils could reach 96%. This reaction system shows the powerful capability of sulfur removal with high S-content oil which was scarcely reported before.

Effect of different substrates on sulfur removal

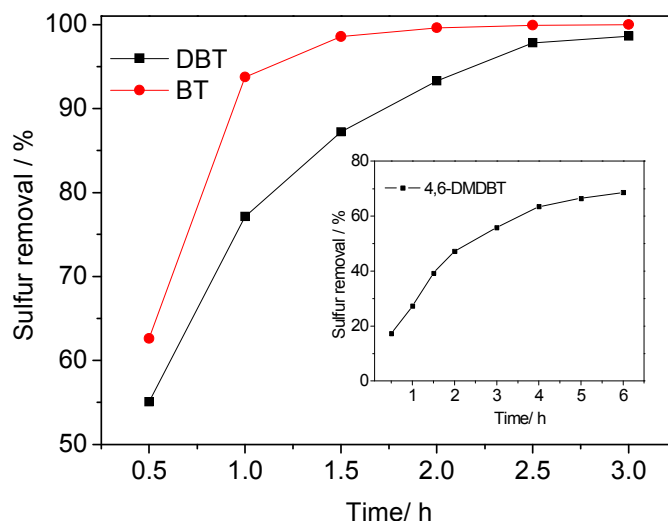


Fig. 7 Effect of different substrates on sulfur removal.

Experiment condition: $T=30^{\circ}\text{C}$, $V(\text{model oil})=15\text{ mL}$, $V(\text{IBA})=250\ \mu\text{L}$,
 $V(\text{DES})=3\text{ mL}$, $v(\text{air})=5\text{ mL/min}$

Different structure of S-containing substrates was also an important factor which would influence the sulfur removal efficiency. Thus, other two main refractory thiophenic sulfur, BT and 4,6-DMDBT, were also investigated in the same reaction conditions. Sulfur removals of BT, DBT and 4,6-DMDBT reached 100, 98.6 and 68.6% at 30°C , respectively, decreasing in the order of $\text{BT} > \text{DBT} > 4,6\text{-DMDBT}$ which is different from many other reported reaction systems⁶⁸⁻⁷⁰. Here, we proposed the reason as following. The active oxygen species in this reaction system, peroxy isobutyrate, was much bigger than many other common seen small species (*e. g.* $\cdot\text{OH}$, $\text{O}_2^{\cdot-}$). The big peroxy isobutyrate may hard to get in touch with S atom in the thiophene ring when two methyl groups emerge. Thus, sulfur removal of 4,6-DMDBT was much lower than that of DBT. Similarly, peroxy isobutyrate may easier to reach

to the S atom in BT, as only one benzene ring exist in this sulfur compound compared to DBT. Finally, sulfur removal of different sulfur compounds decreased in the order of BT > DBT > 4,6-DMDBT.

Effects of fuel composition

The composition of real fuel oil is complicated, including olefins, aromatics and so on. The perfect sulfur removal efficiency with model oil may exhibit not well desulfurization in real fuel oil.⁷¹ To deep understand the above puzzle problem, the effect of fuel oil composition was further studied. Olefins and aromatics are the two main major types of hydrocarbons present in gasoline except the saturated (C₅-C₁₂) alkanes. Here, cyclohexene and paraxylene were chosen as representative compounds and added into the model oil, respectively, to investigate their effects on sulfur removal. The effect of cyclohexene addition at different concentration in model oil is shown in Fig. 8. The final sulfur removals after 3 h reaction were 98.6%, 93.1% and 64.4% with none, 1 wt% and 5 wt% cyclohexene addition, respectively. Sulfur removal decreased much with the concentration of cyclohexene increasing. Cyclohexene, as an unsaturated cyclic olefin, may not only absorb UV light but also easy to be oxidized. The above two reasons led to a negative influence on the oxidation of sulfur compounds. The effect of the aromatics (paraxylene) addition at different concentration in model oil is shown in Fig 9. The final sulfur removals after 3 h reaction were 98.6%, 97.3% and 95.3% with none, 1 wt% and 5 wt% paraxylene addition, respectively. Sulfur removal decreased little with the concentration of

paraxylene increasing. Though paraxylene is hard to oxidize in this environment, it could absorb UV light which may have a negative influence on the oxidation of sulfur compounds. These results indicated that olefins and aromatics can produce the inhibiting effect in photo-oxidative desulfurization process, rising with an increase in the concentration of the inhibiting compounds in the model oil. Based on these finds, we think that optimization of reaction conditions could be taken to mitigate the inhibiting effect of olefins and aromatics in EPODS, which will be the striving direction in the future.

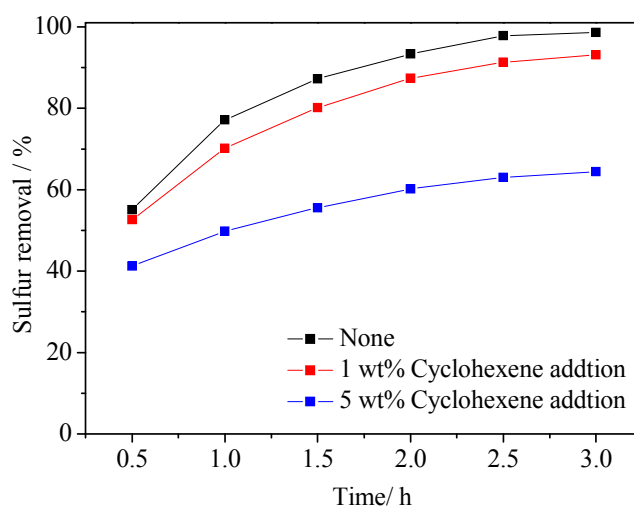


Fig. 8 Effect of additional cyclohexene at various concentrations (wt%) in the model oil.

Experiment condition: $T=30^{\circ}\text{C}$, $V(\text{model oil})=15\text{ mL}$, $V(\text{IBA})=250\ \mu\text{L}$,
 $V(\text{DES})=3\text{ mL}$, $v(\text{air})=5\text{ mL/min}$

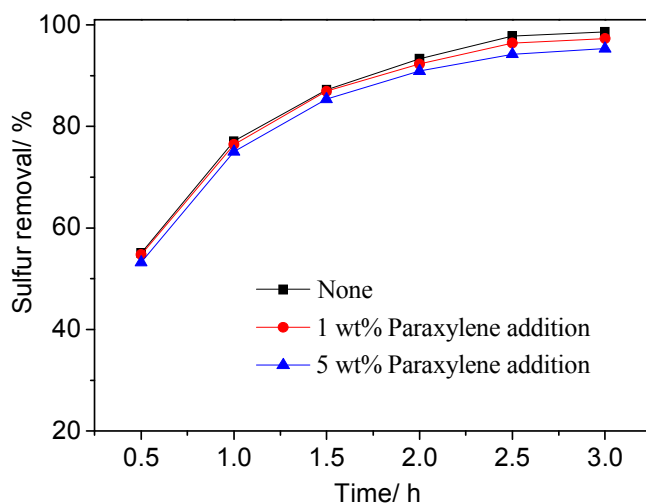


Fig. 9 Effect of additional paraxylene at various concentrations (wt%) in the model oil.
 Experiment condition: $T=30^{\circ}\text{C}$, $V(\text{model oil})=15\text{ mL}$, $V(\text{IBA})=250\ \mu\text{L}$,
 $V(\text{DES})=3\text{ mL}$, $v(\text{air})=5\text{ mL/min}$

Possible mechanism of the DBT photochemical oxidation process

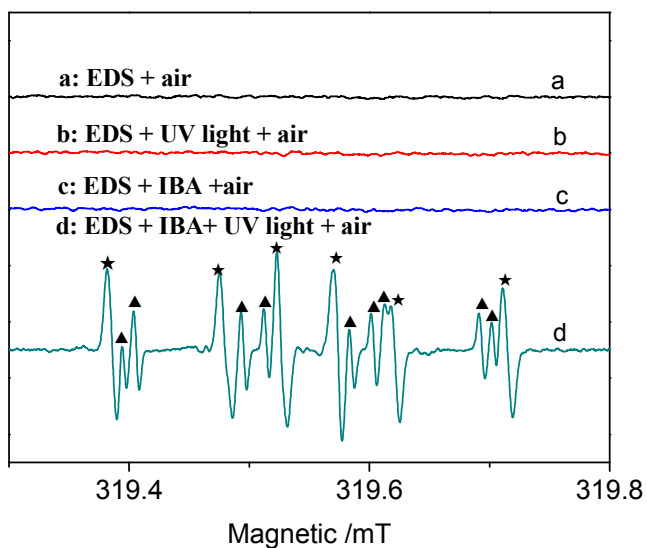


Fig.10 ESR spectra of $\text{DMPO}-(\text{CH}_3)_2\text{CHC}(\text{O})\cdot$ (★) or $\text{DMPO}--(\text{CH}_3)_2\text{CHC}(\text{O})\text{OO}\cdot$ (▲) in IBA/DES/UV light system.

In order to understand the reaction mechanism of PCODS, ESR signals of different reaction systems were detected with the spin trap

5,5-dimethyl-1-pyrroline-N-oxide (DMPO) as shown in Fig. 10. Signals appear only in the system of DES+IBA+UV light. In the systems of DES, DES+UV light and DES+IBA, no obvious signals were detected. From this four detection results, we could indicate that radicals were produced from IBA under UV irradiation. Two groups of characteristic peaks were detected in the systems of DES+IBA+UV light. They were marked as symbols of ★ and ▲, respectively. The six peaks characteristic peaks (★) were typical DMPO-RO• peaks which were corresponded to $(\text{CH}_3)_2\text{CHC}(\text{O})\cdot$ radicals produced from IBA under UV irradiation.^{72, 73} Another nine characteristic peaks (▲) were detected, which were attributed to the characteristic peaks from DMPO-ROOO•. However, DMPO-ROOO• characteristic peaks have twelve according to the literature^{72, 73}. Lack of three peaks maybe because they were covered by the strong six characteristic peaks of $(\text{CH}_3)_2\text{CHC}(\text{O})\cdot$. Combined with the data of desulfurization, ROOO• should be the active oxidizing species and the oxygen played an important role in PCODS.

In order to reach a deep understanding of the mechanism, density functional theory (DFT) was employed to investigate the initial step of the reaction. It was well known that isobutyraldehyde radical ($\text{R-CO}\cdot$) would be easily formed during a photochemical process. The next problem was whether the $\text{R-COOO}\cdot$ radical could be formed in the oxygen environment ($\text{RCO}\cdot + \text{O}_2 = \text{RCOOO}\cdot$). We employed the B3LYP hybrid functional as well as a basis set of 6-31G(d) to explore this reaction. It was interesting to find that the transition state of this reaction could not be located. Hence, a potential energy profile was scanned along with the distance of C-O (O was

from the oxygen molecule). The distance of C-O ranged from 4.3Å to 1.3Å which would cover the main potential energy surface. It can be seen from the Fig. S9 that the potential energy of this system decreases while the distance of C-O decreases (from 4.3Å to 1.5Å). There is no energy increasing along this reaction coordinate that means there is no transition state for this reaction. It is consistent with the result of transition state search. Above discussions of the initial step of photochemical desulfurization further indicated that the $\text{RCOOO}\cdot$ will be readily formed in the oxygen environment.

Sulfur removal of DBT with different aldehydes

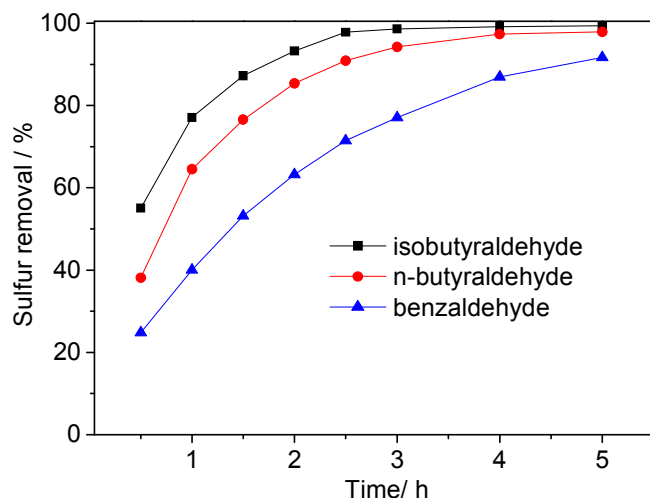
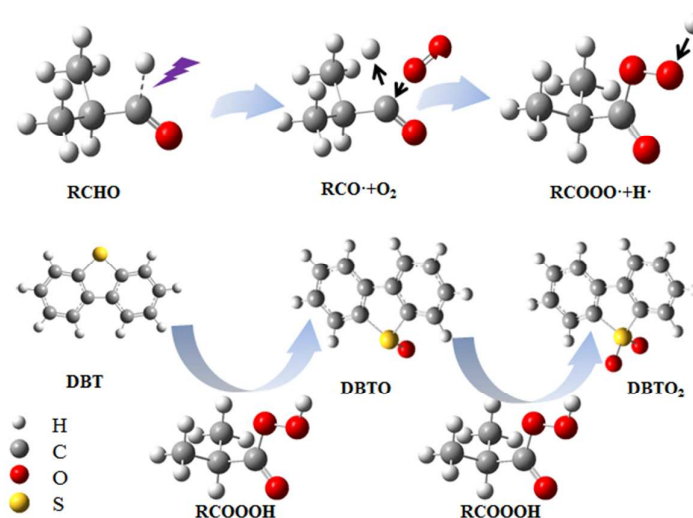


Fig. 11 Sulfur removal of DBT with different aldehydes

Experiment condition: $T=30^{\circ}\text{C}$, $V(\text{model oil})=15\text{ mL}$, $V(\text{aldehyde})=200\ \mu\text{L}$, $t=3\text{ h}$,
 $V(\text{DES})=3\text{ mL}$, $v(\text{air})=5\text{ mL/min}$

In order to further prove this reaction mechanism, the relationship between the structure of aldehyde and desulfurization efficiency, different aldehydes were added into the reaction system under the same experiment conditions. Sulfur removal with

different aldehyde versus reaction time was displayed in Fig. 11. Sulfur removal decreased as: IBA > n-butyraldehyde > benzaldehyde. This may result from following two reasons. First of all, the acyl radical with tertiary α -carbon formed from IBA was more stable than other acyl radicals.⁷⁴ Secondly, the C-H bond energy in formyl group of IBA (364.5 kJ/mol)⁷⁵ was less than that of n-butyraldehyde (371.2 kJ/mol)⁷⁵, which makes $(\text{CH}_3)_2\text{CHCO}\cdot$ easier to be generated than $\text{CH}_3\text{CH}_2\text{CH}_2\text{CO}\cdot$. For benzaldehyde, though the C-H bond energy in formyl group (about 371.1 kJ/mol⁷⁶) was closed to that of n-butyraldehyde, the benzene ring in benzaldehyde could absorb UV light greatly which may make less acyl radical to be formed. Thus, sulfur removals of three aldehydes decreased as: IBA > n-butyraldehyde > benzaldehyde.



Scheme 1. A possible reaction mechanism for the DBT photochemical oxidation process

Based on the above ESR and DFT results, possible reaction route was proposed as shown in Scheme 1. In beginning of this reaction, acyl radical was formed after a proton dissociated from the aldehyde under UV irradiation. Then a peroxy radical was

formed easily by the reaction of acyl radical and molecule oxygen. After this, peroxy radical react with aldehyde, and peracid and acyl radical were generated finally. Hereafter, the new generated acyl radical would reaction with molecule oxygen in the same way. Thus a chain reaction system was established. DBT was first oxidized to sulfoxide by peracid. Then the sulfoxide was further oxidized by peracid and finally converted to sulfone. To further verified speculation, the reaction products of DBT were detected by GC-MS.

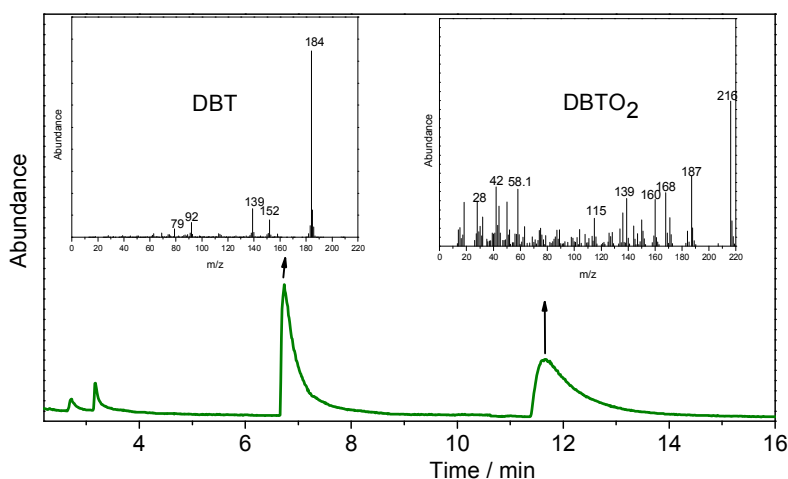


Fig. 12 The GC-MS of product of DBTO₂.

In the reaction process, the DES phase was separated and extracted with carbon tetrachloride. Then carbon tetrachloride phase was collected to study the photochemical oxidizing products by GC-MS. As shown in Fig. 12, there were two main peaks in the total ion chromatogram. The molecular ion peak of mass spectrum of the two main peaks showed at m/z 184 and m/z 216, which were corresponded to the DBT and DBTO₂, respectively. All this can prove that DBT was oxidized to

corresponding sulfone (DBTO₂), which was consistent with our proposal before.

Conclusions

In summary, a simple liquid–liquid extraction and photochemical oxidative desulfurization system (EPODS) composed of air, IBA, and DES for the deep removal of sulfur compounds in model oil has been developed. EDSs were successfully synthesized by a cheap and biodegradable choline chloride (ChCl) and a series of straight-chain monobasic acids. Sulfur compounds in model oil were extracted into DES phase and oxidized to their corresponding sulfones by air under UV irradiation, achieving deep desulfurization. Sulfur removals of BT, DBT and 4,6-DMDBT were 100, 98.6 and 68.6% in the optimized reaction environment, respectively. Finally, the proposed reaction mechanism was proved by ESR, DFT and GC-MS. The features of one-pot extraction combined with metal-free photochemical aerobic oxidative desulfurization in low-cost and greener DES make this reaction potentially promising for practical applications.

Experimental

Materials

All chemicals used in our experiments were of analytical reagent grade without further purification. DBT, benzothiophene (BT), 4, 6-dimethyldibenzothiophene (4, 6-DMDBT) were purchased from Sigma–Aldrich Co., Ltd. IBA was purchased from

Aladdin Industrial Corporation. Other chemical reagents were purchased from Sinopharm Chemical Reagent Co., Ltd.

Characterization and analysis

The FT-IR spectra (KBr disc) were recorded on a Nicolet Model Nexus 470 FT-IR instrument. Elementary analyses were performed with CHN-O-Rapid (Heraeus Corporation). NMR was recorded on an avance II400 MHz Bruker NMR spectrometer. Dimethyl sulfone (DMSO) containing an internal standard TMS was used as solvent. X-band electron spin resonance (ESR) spectra were recorded at ambient temperature on a JES FA200 spectrometer. Gas Chromatography (GC) (Agilent 7890A, HP-5 column, 30 m long \times 0.32 mm inner diameter (id) \times 0.25 μ m film thickness) with an flame ionization detector (FID) and gas chromatograph–mass spectrometer (GC-MS) (Agilent 7890/5975C-gas chromatography (GC)/mass selective detector (MSD), HP-5 MS column, 30 m \times 250 μ m i.d. \times 0.25 μ m) were used.

Synthesis of DESs and model oil

Choline chloride (ChCl) and organic acids were added to a 100 mL round-bottomed flask at the molar ratio of 1:2. Two raw composites become liquid phase and were stirred vigorously in oil bath with a magnetic stirrer (800 r/min) at the temperature of 80°C for 3 h. After reaction, the homogeneous colorless liquid was cooled to room temperature naturally.

Three thiophene analogue sulfur compounds, BT, DBT and 4, 6-DMDBT were chosen as typical sulfur-containing compounds in fuels. Then they were dissolved in n-octane as model oil, with S-content of 500 ppm. Model oils with different DBT

concentration, 600, 800, 1000 ppm were also prepared in the same way. Tetradecane was used as internal standard.

Photochemical oxidative desulfurization process

3 mL DES and 15 mL model oil were added into a home-made 30 mL two-necked flask and fresh air was introduced to the system by an air pump with the airflow velocity of 5 mL/min. Here, a super-heated water bath was used to keep a constant reaction temperature. Then certain amount of aldehyde was injected into the reaction system after extraction for 20 min. The mixture was stirred for 3 h under UV irradiation (a 250 W high pressure Hg lamp). The picture of reaction equipment was shown in Scheme S1.

The reaction solution samples were collected every 20 min and analyzed by GC-FID by the micro-injector to evaluate the sulfur content in the system. The conversion of DBT, BT and 4, 6-DMDBT in the model oil was used to indicate the removal of sulfur compounds. The temperature of the GC process started at 100°C and rose to 200°C at 15°C•min⁻¹. Injector temperature was 300°C and detector temperature was 250°C.

Acknowledgements

This work was financially supported by the National Nature Science Foundation of China (Nos. 21376111, 21276117, 21076099) and Postdoctoral Foundation of China (No. 2014M551516).

References:

1. R. Martinez-Palou and R. Luque, *Energ. Environ. Sci.*, 2014, **7**, 2414-2447.
2. W. S. Zhu, B. L. Dai, P. W. Wu, Y. H. Chao, J. Xiong, S. H. Xun, H. P. Li, H. M. Li, *ACS Sustain. Chem. Eng.* 2015, **3**, 186-194.
3. F. T. Li, R. H. Liu, J. H. Wen, D. S. Zhao, Z. M. Sun and Y. Liu, *Green Chem.*, 2009, **11**, 883-888.
4. H. Y. Lü, Y. N. Zhang, Z. X. Jiang and C. Li, *Green Chem.*, 2010, **12**, 1954-1958.
5. H. S. Gao, C. Guo, J. M. Xing, J. M. Zhao and H. Z. Liu, *Green Chem.*, 2010, **12**, 1220-1224.
6. W. H. Lo, H. Y. Yang and G. T. Wei, *Green Chem.*, 2003, **5**, 639-642.
7. W. S. Zhu, J. T. Zhang, H. M. Li, Y. H. Chao, W. Jiang, S. Yin H. Liu, *RSC Adv.*, 2012, **2**, 658-664.
8. J. Xiao, L. M. Wu, Y. Wu, B. Liu, L. Dai, Z. Li, Q. B. Xia and H. Xi, *Appl. Energy*, 2014, **113**, 78-85.
9. L. Alonso, A. Arce, M. Francisco, O. Rodriguez and A. Soto, *AIChE J.*, 2007, **53**, 3108-3115.
10. A. Bosmann, L. Datsevich, A. Jess, A. Lauter, C. Schmitz and P. Wasserscheid, *Chem. Commun.*, 2001, 2494-2495.
11. C. H. Shu, T. H. Sun, Q. B. Guo, J. P. Jia and Z. Y. Lou, *Green Chem.*, 2014, **16**, 3881-3889.
12. J. M. Palomino, D. T. Tran, J. L. Hauser, H. Dong and S. R. J. Oliver, *J. Mater.*

- Chem. A*, 2014, **2**, 14890-14895.
13. Y. W. Shi, X. W. Zhang, L. Wang and G. Z. Liu, *AIChE J.*, 2014, **60**, 2747-2751.
 14. Y. S. Shen, P. W. Li, X. H. Xu and H. Liu, *RSC Adv.*, 2012, **2**, 1700-1711.
 15. E. Kianpour and S. Azizian, *Fuel*, 2014, **137**, 36-40.
 16. P. Verdia, E. J. Gonzalez, B. Rodriguez-Cabo and E. Tojo, *Green Chem.*, 2011, **13**, 2768-2776.
 17. J. J. Gao, H. Meng, Y. Z. Lu, H. X. Zhang and C. X. Li, *AIChE J.*, 2013, **59**, 948-958.
 18. S. Aggarwal, I. A. Karimi and G. R. Ivan, *Mol. Biosyst.*, 2013, **9**, 2530-2540.
 19. W. S. Zhu, H. M. Li, Q. Q. Gu, P. W. Wu, G. P. Zhu, Y. S. Yan, G. Y. Chen, *J. Mol. Catal. A: Chemical*, 2011, **336**, 16-22.
 20. Y. S. Chi, C. P. Li, Q. Z. Jiao, Q. S. Liu, P. F. Yan, X. M. Liu and U. Welz-Biermann, *Green Chem.*, 2011, **13**, 1224-1229.
 21. J. Zhang, J. P. Li, T. J. Ren, Y. H. Hu, J. J. Ge and D. S. Zhao, *RSC Adv.*, 2014, **4**, 3206-3210.
 22. H. Y. Lü, J. B. Gao, Z. X. Jiang, Y. X. Yang, B. Song and C. Li, *Chem. Commun.*, 2007, 150-152.
 23. X. R. Zhou, J. Li, X. N. Wang, K. Jin and W. Ma, *Fuel Process. Technol.*, 2009, **90**, 317-323.
 24. W. Zhang, H. Zhang, J. Xiao, Z. X. Zhao, M. X. Yu and Z. Li, *Green Chem.*, 2014, **16**, 211-220.

25. Z. E. A. Abdalla and B. S. Li, *Chem. Eng. J.*, 2012, **200**, 113-121.
26. Q. Lü, G. Li and H. Y. Sun, *Fuel*, 2014, **130**, 70-75.
27. X. T. Wang, W. Chen and Y. F. Song, *Eur. J. Inorg. Chem.*, 2014, **2014**, 2779-2786.
28. J. Zhang, A. J. Wang, Y. J. Wang, H. Y. Wang and J. Z. Gui, *Chem. Eng. J.*, 2014, **245**, 65-70.
29. W. Jiang, W. S. Zhu, H. M. Li, Y. H. Chao, S. H. Xun, Y. H. Chang, H. Liu, Z. Zhao, *J. Mol. Catal. A: Chemical*, 2014, **382**, 8-14.
30. C. H. Ma, B. Dai, P. Liu, N. Zhou, A. J. Shi, L. L. Ban and H. W. Chen, *J. Ind. Eng. Chem.*, 2014, **20**, 2769-2774.
31. J. L. Wang, D. S. Zhao and K. X. Li, *Energ. Fuel.*, 2010, **24**, 2527-2529.
32. W. Guo, C. Y. Wang, P. Lin and X. P. Lu, *Appl. Energ.*, 2011, **88**, 175-179.
33. P. F. Zhang, Y. Wang, H. R. Li and M. Antonietti, *Green Chem.*, 2012, **14**, 1904-1908.
34. N. F. Tang, Y. N. Zhang, F. Lin, H. Y. Lü, Z. X. Jiang and C. Li, *Chem. Commun.*, 2012, **48**, 11647-11649.
35. J. T. Sampanthar, H. Xiao, H. Dou, T. Y. Nah, X. Rong and W. P. Kwan, *Appl. Catal. B-Environ.*, 2006, **63**, 85-93.
36. F. Lin, D. E. Wang, Z. X. Jiang, Y. Ma, J. Li, R. G. Li and C. Li, *Energ. Environ. Sci.*, 2012, **5**, 6400-6406.
37. F. Lin, Y. N. Zhang, L. Wang, Y. L. Zhang, D. E. Wang, M. Yang, J. H. Yang, B. Y. Zhang, Z. X. Jiang and C. Li, *Appl. Catal. B-Environ.*, 2012, **127**,

- 363-370.
38. R. Vargas and O. Nunez, *J. Mol. Catal. A-Chem.*, 2008, **294**, 74-81.
39. X. J. Wang, F. T. Li, J. X. Liu, C. G. Kou, Y. Zhao, Y. J. Hao and D. S. Zhao, *Energ. Fuel.*, 2012, **26**, 6777-6782.
40. W. S. Zhu, Y. H. Xu, H. M. Li, B. L. Dai, H. Xu, C. Wang, Y. H. Chao and H. Liu, *Korean J. Chem. Eng.*, 2014, **31**, 211-217.
41. T. H. T. Vu, T. T. T. Nguyen, P. H. T. Nguyen, M. H. Do, H. T. Au, T. B. Nguyen, D. L. Nguyen and J. S. Park, *Mater. Res. Bull.*, 2012, **47**, 308-314.
42. C. Wang, W. S. Zhu, Y. H. Xu, H. Xu, M. Zhang, Y. H. Chao, S. Yin, H. M. Li and J. G. Wang, *Ceram. Int.*, 2014, **40**, 11627-11635.
43. F. T. Li, Y. Liu, Z. M. Sun, Y. Zhao, R. H. Liu, L. J. Chen and D. S. Zhao, *Catal. Sci. Technol.*, 2012, **2**, 1455-1462.
44. W. S. Zhu, H. M. Li, X. Jiang, Y. S. Yan, J. D. Lu, L. N. He and J. X. Xia, *Green Chem.*, 2008, **10**, 641-646.
45. J. Xiong, W. S. Zhu, H. M. Li, Y. H. Xu, W. Jiang, S. H. Xun, H. Liu and Z. Zhao, *AIChE J.*, 2013, **59**, 4696-4704.
46. J. T. Zhang, W. S. Zhu, H. M. Li, W. Jiang, Y. Q. Jiang, W. L. Huang and Y. S. Yan, *Green Chem.*, 2009, **11**, 1801-1807.
47. A. Paiva, R. Craveiro, I. Aroso, M. Martins, R. L. Reis and A. R. C. Duarte, *ACS Sustain. Chem. Eng.*, 2014, **2**, 1063-1071.
48. A. P. Abbott, D. Boothby, G. Capper, D. L. Davies and R. K. Rasheed, *J. Am. Chem. Soc.*, 2004, **126**, 9142-9147.

49. A. M. M. Sousa, H. K. S. Souza, N. Latona, C. K. Liu, M. P. Goncalves and L. Liu, *Carbohydr. Polym.*, 2014, **111**, 206-214.
50. H. G. Morrison, C. C. Sun and S. Neervannan, *Int. J. Pharm.*, 2009, **378**, 136-139.
51. Q. Zeng, Y. Z. Wang, Y. H. Huang, X. Q. Ding, J. Chen and K. J. Xu, *Analyst*, 2014, **139**, 2565-2573.
52. A. P. Abbott, G. Capper, D. L. Davies, K. J. McKenzie and S. U. Obi, *J. Chem. Eng. Data*, 2006, **51**, 1280-1282.
53. S. Q. Xia, G. A. Baker, H. Li, S. Ravula and H. Zhao, *RSC Adv.*, 2014, **4**, 10586-10596.
54. A. P. Abbott, K. El Ttaib, G. Frisch, K. S. Ryder and D. Weston, *Phys. Chem. Chem. Phys.*, 2012, **14**, 2443-2449.
55. A. P. Abbott, K. El Ttaib, G. Frisch, K. J. McKenzie and K. S. Ryder, *Phys. Chem. Chem. Phys.*, 2009, **11**, 4269-4277.
56. M. A. Kareem, F. S. Mjalli, M. A. Hashim and I. M. AlNashef, *J. Chem. Eng. Data*, 2010, **55**, 4632-4637.
57. Q. H. Zhang, K. D. O. Vigier, S. Royer and F. Jerome, *Chem. Soc. Rev.*, 2012, **41**, 7108-7146.
58. M. C. Gutiérrez, D. Carriazo, C. O. Ania, J. B. Parra, M. Luisa Ferrer and F. del Monte, *Energ. Environ. Sci.*, 2011, **4**, 3535-3544.
59. A. Carranza, J. A. Pojman and J. D. Mota-Morales, *RSC Adv.*, 2014, **4**, 41584-41587.

60. F. S. Oliveira, A. B. Pereiro, L. P. N. Rebelo and I. M. Marrucho, *Green Chem.*, 2013, **15**, 1326-1330.
61. W. J. Guo, Y. C. Hou, W. Z. Wu, S. H. Ren, S. D. Tian and K. N. Marsh, *Green Chem.*, 2013, **15**, 226-229.
62. M. Sharma, C. Mukesh, D. Mondal and K. Prasad, *RSC Adv.*, 2013, **3**, 18149-18155.
63. W. Zaidi, A. Boisset, J. Jacquemin, L. Timperman and M. Anouti, *J. Phys. Chem. C*, 2014, **118**, 4033-4042.
64. V. Stepankova, P. Vanacek, J. Damborsky and R. Chaloupkova, *Green Chem.*, 2014, **16**, 2754-2761.
65. Y. C. Zhang, F. L. Lu, X. H. Cao and J. Q. Zhao, *RSC Adv.*, 2014, **4**, 40161-40169.
66. C. P. Li, D. Li, S. S. Zou, Z. Li, J. M. Yin, A. L. Wang, Y. N. Cui, Z. L. Yao and Q. Zhao, *Green Chem.*, 2013, **15**, 2793-2799.
67. H. Y. Lü, S. N. Wang, C. L. Deng, W. Z. Ren and B. C. Guo, *J. Hazard. Mater.*, 2014, **279**, 220-225.
68. M. Zhang, W. S. Zhu, S. H. Xun, H. M. Li, Q. Q. Gu, Z. Zhao and Q. Wang, *Chem. Eng. J.*, 2013, **220**, 328-336.
69. J. Zhang, A. J. Wang, X. Li and X. H. Ma, *J. Catal.*, 2011, **279**, 269-275.
70. Y. Chen and Y. F. Song, *ChemPlusChem*, 2014, **79**, 304-309.
71. W. Zhu, G. Zhu, H. Li, Y. Chao, Y. Chang, G. Chen and C. Han, *Journal of Molecular Catalysis a-Chemical*, 2011, **347**, 8-14.

72. H. M. Li, W. S. Zhu, Y. Wang, J. T. Zhang, J. D. Lu and Y. S. Yan, *Green Chem.*, 2009, **11**, 810-815.
73. W. S. Zhu, W. L. Huang, H. M. Li, M. Zhang, W. Jiang, G. Y. Chen and C. R. Han, *Fuel Process. Technol.*, 2011, **92**, 1842-1848.
74. T. V. Rao, B. Sain, S. Kafola, Y. K. Sharma, S. M. Nanoti and M. O. Garg, *Energ. Fuel.*, 2007, **21**, 3420-3424.
75. V. E. Tumanov, E. A. Kromkin and E. T. Denisov, *Russ. Chem. Bull.*, 2002, **51**, 1641-1650.
76. J. A. M. Simões and D. Griller, *Chem. Phys. Lett.*, 1989, **158**, 175-177.

One-pot extraction combined with metal-free photochemical aerobic oxidative desulfurization in deep eutectic solvent

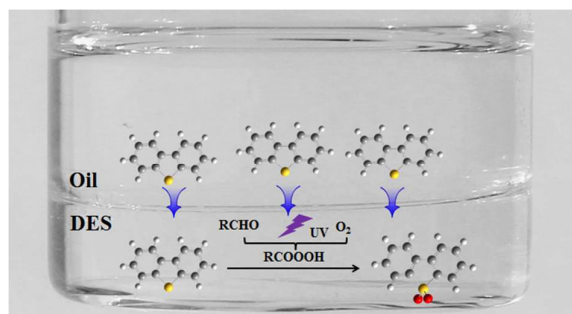
Wenshuai Zhu^{*[a]}, Chao Wang^[a], Hongping Li^[a], Peiwen Wu,^[a] Suhang Xun,^[a] Wei Jiang^[b], Zhigang Chen^[a], Zhen Zhao^[c] and Huaming Li^{*[b]}

^[a]School of Chemistry and Chemical Engineering, Jiangsu University, 301 Xuefu Road, Zhenjiang 212013 (P. R. China)

^[b] Insititute for Energy Research, Jiangsu University, 301 Xuefu Road, Zhenjiang 212013 (P. R. China)

^[c] State Key Laboratory of Heavy Oil Processing, Faculty of Science, China University of Petroleum, Beijing 102249 (P. R. China)

E-mail: zhuws@ujs.edu.cn (W.S. Zhu) , lihm@ujs.edu.cn (H.M. Li)



One-pot extraction combined with metal-free photochemical aerobic oxidative deep desulfurization of fuels in deep eutectic solvents was successfully achieved.